GPO PRICE $ _____

CFSTI PRICE(S) $ _____

Hard copy (HC) $2.00

Microfiche (MF) .50

ff 653 July 65

FACILITY FORM 602

N66 24549 (ACCESSION NUMBER) (THRU)

31 (PAGES) (CODE)

CR-74582 (NASA CR OR TMX OR AD NUMBER) 13 (CATEGORY)

GCA CORPORATION

Bedford, Massachusetts

NATIONAL AERONAUTICS AND SPACE ADMINISTRATION
GODDARD SPACE FLIGHT CENTER
Greenbelt, Maryland

January 1966

GCA CORPORATION
GCA TECHNOLOGY DIVISION
Bedford, Massachusetts

SODIUM VAPOR EXPERIMENT

Quarterly Progress Report No. 2

Covering the Period
1 October 1965 - 31 December 1965

Prepared under Contract No. NAS5-3970

TABLE OF CONTENTS

I. INTRODUCTION

The objective of this contract and the methods employed were discussed in the first quarterly progress report. The major effort during this reporting period was preparation for the firing of five Nike-Apache vapor payloads from Wallops Island during January 1966. Section II of this report discusses the purpose and preparations for these firings.

Subsequent sections of this report contain discussion of some aspects of the general atmospheric dynamics in the E-region (Section III) and a preliminary analysis of the irregular structure in vapor trails below about 105 km which has raised the question of pre-existing atmospheric turbulence (Section IV). Section V contains the plans for work during the next reporting period.

II. PURPOSE AND PROGRAM FOR THE JANUARY 1966 ROCKET FIRINGS AT WALLOPS ISLAND

Time variations of winds which have been obtained from previous observations indicate that sequential firings spaced as close as an hour or so may be desirable in order to determine the exact nature of the variations. The schedule of the January series at Wallops Island was selected for this purpose. The series will begin with an alkali-vapor trail during evening sunset and will be followed by three TMA trails at intervals of 1-1/2 hr, 1-1/2 hr, and 3 hr. The final trail will be alkali-vapor during morning twilight which is about six hours after the last TMA trail. A back-up rocket will be available in case of difficulty with any of the vehicle or payloads. Preparation of two alkali-vapor payloads and four TMA payloads was completed during this period.

Photographic equipment for four camera sites was prepared and tested. The standard 70 mm cameras are to be used as primary recorders for the twilight trails. A less sophisticated but higher speed 70 mm camera has been prepared for the night time TMA trails. The system can be simpler than the standard twilight cameras since precise shutter action is not necessary due to the low sky background at night, and star images can be obtained on every frame. This eliminates the need for fiducial lights and precision mounts. Long focal length (20 in.) lenses will be used on K-24 cameras at each site except Dover which will have a 36 in. lens. These cameras will record the formation and growth of the trails around 100 km where small scale structure and high growth rates are usually present. Detailed observations will be helpful in the determination of the nature and origin of this phenomenon.

III. DISCUSSION

The wind-profiles obtained from rocket-laid vapor trails usually cover the height-range of 80 to 130 km. A few extend as low as 70 km and several extend beyond 160 km. A useful two-dimensional representation of the data is the hodograph. A polar plot of the magnitude and direction of the horizontal wind vector at each height is first constructed, and the hodograph is obtained from a continuous arc drawn through points representing consecutive heights.

An examination of the hodographs of the trails that have been analyzed so far reveals a number of recurring features. The most striking of these is that, to a first approximation, the hodograph can be described as a spiral. The sense of rotation of this spiral, as one follows it from its minimum to its maximum height, is clockwise. (These data pertain to the northern hemisphere; meteor data from the southern hemisphere reveal a counter-clockwise rotation.) A particular hodograph never attains the idealization of a smooth spiral throughout its height-range. Over height-intervals of a few kilometers the spiral is usually interrupted by arcs, whose sense of rotation is arbitrary. The points where such intervals join each other or at the spiral portion of the hodograph have the appearance of cusps or corners. Nevertheless, large segments of a smooth, clockwise spiral, corresponding to intervals of from 10 to 20 km, are never completely absent. This is especially true of the region above 120 km.

A second feature of the hodograph is the inverse relationship between the magnitude of the wind and the number of corners present. Whenever the hodograph resembles a smooth, continuous spiral, the magnitude of the winds

associated with it is large. Conversely, the presence of a large number of corners is associated with winds of small magnitude.

The similarity between the hodographs and a continuous spiral suggests strongly that this region of the atmosphere responds as a whole to a disturbance due to a single source. Moreover, the sense of rotation indicates a disturbance that is propagating predominantly upward.

Most of the existing data provide only a vertical profile of the horizontal wind at a given instant and at a given location. The data contained no information concerning the temporal variation of the wind-profile or the horizontal components of the gradient of the wind. Some profiles are approximately 12 hours apart (corresponding to consecutive evening and morning twilight). In a few instances profiles were measured simultaneously at sites separated by a few hundred kilometers, or a few hours apart at the same location. These yield some preliminary information about the horizontal and temporal variation of wind-profiles.

Quite obviously, the full explanation of the observed winds cannot rest on evidence supplied by the winds alone. At this time, however, the thermodynamic variables (pressure, density, and temperature) in the region of interest are established reasonably well only in an average way. Moreover, the concentrations of the atomic and molecular constituents, on which the heating and the cooling rates depend sensitively, are still uncertain. Thus, at present, the existing information can only help indicate a suitable mathematical model and provide an estimate of the various quantities appearing in the equations.

The required equations are those for the determination of the dynamics, the description of the conservation of mass, and the determination of the changes in entropy. They are, respectively:

$$\frac{\partial \vec{u}}{\partial t} + \vec{u} \cdot \nabla \vec{u} + \frac{1}{\rho} \nabla p + \nabla X + 2\vec{\Omega} \times \vec{u} = \vec{f} \qquad (1)$$

$$\frac{\partial \rho}{\partial t} + \nabla \cdot (\rho \vec{u}) = 0 \qquad (2)$$

$$\left(\frac{\partial \rho}{\partial t} + \vec{u} \cdot \nabla p\right) - c^2 \left(\frac{\partial \rho}{\partial t} + \vec{u} \cdot \nabla p\right) = \frac{\rho\, a c^2}{C_p} q \qquad (3)$$

where $\vec{u}$ = velocity vector

ρ = density

p = pressure

X = geopotential

$\vec{\Omega}$ = Coriolis vector

c = speed of sound

C_p = specific heat (constant pressure)

a = coefficient of thermal expansion

$\vec{f}$ = force per unit volume due to all sources

q = net gain of heat per unit mass and per unit time.

In the region of interest the equation of state is given by the ideal gas law

$$p = \frac{R_o M_o}{M} \rho T \qquad (4)$$

where T = temperature

R_o = the universal gas constant

M = mean molecular weight

M_o = value of M at sea-level

Equation (3), with the help of the definitions of c, a, and C_p, may be written as

$$\left(\frac{\partial}{\partial t} + \vec{u} \cdot \nabla \right) \ln \left(\frac{p}{\rho \gamma} \right) = (\gamma - 1) \frac{\rho}{p} q \qquad (5)$$

where γ is the ratio of specific break.

The vector Equation (1) can be decomposed into three equations for the zonal (eastward), meridional (southward), and vertical (upward) components, denoted by u_ϕ, u_θ, and u_r, respectively. In spherical polar coordinates these equations are:

$$\frac{\partial u_\phi}{\partial t} + u_r \frac{\partial u_\phi}{\partial r} + \frac{u_\theta}{r} \frac{\partial u_\phi}{\partial \theta} + \frac{u_\phi}{r \sin \theta} \frac{\partial u_\phi}{\partial \phi} + \frac{u_r}{r} u_\phi + \frac{u_\phi \cot \theta}{r} u_\theta$$

$$+ \frac{1}{\rho} \frac{1}{r \sin \theta} \frac{\partial p}{\partial \phi} + 2\Omega (\cos \theta \, u_\theta + \sin \theta \, u_r) = f_\phi \qquad (6)$$

$$\frac{\partial u\theta}{\partial t} + u_r \frac{\partial u\theta}{\partial r} + \frac{u\theta}{r} \frac{\partial u_\theta}{\partial \theta} + \frac{u_\theta}{r} \frac{\partial u_\theta}{\partial \theta} + \frac{u_\phi}{r \sin \theta} \frac{\partial u_\theta}{\partial \phi} + \frac{u_r}{r} u_\theta - \frac{u\phi \cot \theta}{r} u_\phi$$

$$+ \frac{1}{\rho} \frac{1}{r} \frac{\partial p}{\partial \theta} - 2\Omega \cos \theta \, u_\phi = f_\theta \qquad (7)$$

$$\frac{\partial u_r}{\partial t} + u_r \frac{\partial u_r}{\partial r} + \frac{u\theta}{r} \frac{\partial u_r}{\partial \theta} + \frac{u_\phi}{r \sin \theta} \frac{\partial u_r}{\partial \phi} - \frac{(u_\theta^2 + u_\phi^2)}{r} + \frac{1}{\rho} \frac{\partial p}{\partial r} + \frac{\partial \chi}{\partial r} - 2\Omega \sin \theta u_\phi = fr$$

(8)

In these equations θ is the colatitude (measured from the north pole), and r is the radial distance from the center of the earth. It is useful to establish, insofar as possible, the order of magnitude of each term appearing in Equation (6).

The time required for u_ϕ to change significantly is certainly longer than 15 minutes (the time interval during which a vapor-trail remains observable). On the other hand, wind-profiles measured four hours apart show that the profile has altered significantly. Thus, a characteristic time is about two to three hours. In units of meter-sec^{-2} adopted for each term of Equation (6), the magnitude of the first term is given by

$$\frac{\partial u_\phi}{\partial t} \approx (1 \rightarrow 2) \times 10^{-4}\, u_\phi$$

The vapor-trail method does not provide direct measurements of vertical velocities. Meteor data, however, reveal a vertical velocity of a few meters per second around 100 km. The vertical shear, that is, the vertical derivative of a wind component, can be calculated easily from the wind-profile. At 100 km the vertical shear may be anywhere between 10 and 100 meters/sec/km (10^{-2} and 10^{-1} sec^{-1}). For the magnitude of the second term in Equation (6) we then have

$$u_r \frac{\partial u_\phi}{\partial r} \approx (1 \rightarrow 2\ msec^{-1}) \times (10^{-2} \rightarrow 10^{-1}\ sec^{-1}) = (10^{-2} \rightarrow 2\times10^{-1})\, sec^{-1}$$

At present there is very limited data on the horizontal variation of winds at the same instant. We base our estimate on the data from three trails separated by about 2000 km along a north-south direction. These show variations ranging between 10 percent and 20 percent in the three profiles. If similar variations are assumed in the east-west direction, the magnitude of the third and fourth terms is given by

$$\frac{u_\theta}{r} \frac{\partial u_\theta}{\partial \theta} \approx \frac{u_\phi}{r \sin\theta} \frac{\partial u_\phi}{\partial \phi} \approx (5 \rightarrow 10) \times 10^{-5}\, u_\phi$$

The fifth term is negligible:

$$\frac{u_r}{r} u_\phi \approx 10^{-7} u_\phi$$

The sixth term is, for middle latitudes:

$$\frac{u_\phi \cot \theta}{r} u_\theta \approx (1 \rightarrow 2) \times 10^{-5} u_\phi$$

At present there exist no data necessary for the evaluation of the seventh term (containing the zonal pressure gradient). An uncertain estimate may be obtained as follows. Assume that the pressure undergoes a diurnal variation due to solar heating. This time-variation can be converted into a zonal variation by the further assumption that it represents a traveling disturbance. Then

$$\frac{\partial p}{\partial \phi} = \frac{1}{r} \frac{\partial p}{\partial t}$$

Let us now suppose that, for Δt = 12 hours $\simeq 4 \times 10^4$ sec,

$$\Delta p \approx \alpha p = \alpha \rho g H,$$

where H is the scale height and α represents the percent pressure variation. Then for middle latitudes

$$\frac{1}{\rho} \frac{1}{r \sin \theta} \frac{\partial p}{\partial \phi} \approx \frac{\alpha g H}{(r\Omega \sin \theta) \Delta t} \approx 6 \times 10^{-4} \alpha H$$

with H in units of kilometers. Hence, this term is about $4 \times 10^{-3} \alpha$ (m/sec^2) at 100 km and about $10^{-2} \alpha$ (m/sec^2) at 130 km. If this argument is valid, then normal, (that is, quasi-periodic) pressure variations are too small to generate the observed winds locally in the

region of 80 to 130 km. Nonetheless, at higher levels the normal pressure gradients become increasingly important. At the same time, the presence and persistence (in time) of corners in the wind profile suggest that pressure fluctuations, other than the quasi-periodic ones, can occur. This aspect of the problem requires further clarification.

The eighth term in the equation, due to the Coriolis force, is large, and it can be evaluated readily:

$$2\Omega\ (\cos\theta\ u_\theta + \sin\theta\ u_r) \approx 2\Omega \cos\theta\ u_\theta \approx 10^{-4}\ u_\theta$$

for middle latitudes.

The force term on the right side of Equation (6) is due mostly to molecular viscosity. Since vertical variations are much larger than horizontal variations, this term is, essentially,

$$f_\phi \approx \frac{\eta}{\rho} \frac{\partial^2 u_\phi}{\partial r^2}$$

where η is the coefficient of dynamic viscosity. Its value above 90 km is uncertain. Nevertheless, until a more reliable determination is available values for η can be computed from Sutherland's empirical formula:

$$\eta = \beta T^{1/2}\ (1 + T_o/T)^{-1}$$

where $\beta \simeq 1.5 \times 10^{-5}$ gm sec^{-1} cm^{-1} ($^\circ$K)$^{-1/2}$, and $T_o = 110.4^\circ$K. Except in the vicinity of corners in the hodograph, a rough estimate of the second derivative is given by

$$\frac{\partial^2 u_\phi}{\partial r^2} \approx 2 \times 10^{-7}\, u_\phi \ (m^{-1}\ sec^{-1})$$

using

$$\rho = 5 \times 10^{-5} \text{ gm cm}^{-3},\ \eta = 1.4 \times 10^{-4} \text{ gm sec}^{-1} \text{ cm}^{-1} \text{ at 100 km}$$

and

$$\rho = 7 \times 10^{-12} \text{ gm cm}^{-3},\ \eta = 2.9 \times 10^{-4} \text{ gm sec}^{-1} \text{ cm}^{-1} \text{ at 180 km}$$

we have

$$f_\phi \simeq 6 \times 10^{-6}\, u_\phi \text{ at 100 km}$$

$$\simeq 8 \times 10^{-4}\, u_\phi \text{ at 130 km}$$

Hence, the viscous forces, even away from corners (that is, for normal vertical shears) become important somewhere between 100 and 130 km.

If a value of 50 to 100 meters/second is assigned to u_ϕ, then it is evident that the terms of Equation (6) are comparable in magnitude, with the exception of the fifth term ($u_r\, u_\phi/r$), and of the pressure gradient term in the lower region. In particular the well-established magnitude of the second term ($u_r\, \partial u_\phi/\partial_r$) attests to the essential non-linearity of the equations. This non-linearity is but a mathematical expression of the physical fact that, in the region under consideration, the atmosphere responds non-linearly to the driving forces. Accordingly, attempts to describe the motions of the atmosphere as a super-position of distinct and independent motions are unlikely to give a correct description, even qualitatively.

IV. IRREGULAR TRAIL STRUCTURE AROUND 100 KM

A. VISUAL APPEARANCE OF TRAIL

Above 110 km, alkali vapor trails always appear smooth and diffusion coefficients are in good agreement with the theory of molecular diffusion[1]. Below this height, the trails generally are not smooth in appearance and expand at a rate greater than is expected from molecular diffusion alone. These irregularities have been interpreted by some investigators[2] as pre-existing atmospheric turbulence. Previously, the production of irregular fluctuations of electron density by turbulence was proposed to explain certain rf scattering phenomena associated with the lower E region. Many authors[3] have found the explanation satisfactory and in some cases predicted the character of the turbulence. Close examination of the form and growth of the distorted vapor trails, however, shows that the irregular regions do not have certain characteristics which are generally attributed to hydro-dynamic turbulence.

A photograph of the irregular portion of a typical vapor trail is shown in Figure 1. Two distinct types of structure may be observed to be present. In the region from 109 to 103 km, the structure is "globular" and below 100 km it is "stringy". The 3-km region between these distinctly different types of irregularities appears to have some of the characteristics of both.

This appearance is typical of most trails. However, all trails do not have as much "globular" structure. Table I is a summary of data from all the trails from Wallops Island in which the occurrence or absence of the globules could be determined. It is seen that they occur in the region 100 to

TABLE I

SUMMARY OF OCCURRENCE OF SMALL
SCALE VAPOR TRAIL IRREGULARITIES

Twilight Period	Date	Height on Top of Globules (km)	Change From Globules to Strings (km)	Height Interval (km)	Shear Greater Than 10 m/sec/km	Shear Less Than 10 m/sec/km
PM	18 Nov 1959	93	---	---	---	---
PM	24 May 1960	111	107	4	x	
		103	97	6		x
AM	9 Dec 1960	105	97	8	x	
AM	19 April 1961	104	100	4	x	
PM	20 April 1961	106	96	10	x	
AM	21 April 1961	108	102	6	x	
PM	16 Sept 1961	108	104	4		x
AM	17 Sept 1961	111	100	10	x	
PM	1 March 1962	107	96	11	x	
AM	2 March 1962	104	97	7	x	
PM	23 March 1962	106	102	4	x	
PM	27 March 1962	107	98	7	x	
AM	17 April 1962	107	103	4		x
PM	6 June 1962	101	97	4	---	x
AM	7 Nov 1962	109	101	8	x	
AM	30 Nov 1962	102	100	2	x	
PM	20 Feb 1963	111	109	2		x
		106	96	10	x	
PM	21 Feb 1963	108	105	3	x	
PM	21 May 1963	105	98	7	x	
AM	22 May 1963	99	97	2		x
PM	22 May 1963	99	95	4		x
PM	23 May 1963	104	95	9		x
PM	24 May 1963	105	103	2	x	
PM	15 Jan 1964	100	96	4	x	
AM	16 Jan 1964	109	104	5		x
PM	14 July 1964	106	100	6	x	
AM	15 July 1964	108	101	7		x
PM	7 Oct 1964	102	---	---	x	
AM	8 Oct 1964	Smooth Trail	---	---		
PM	10 Nov 1964	109	101	8	x	

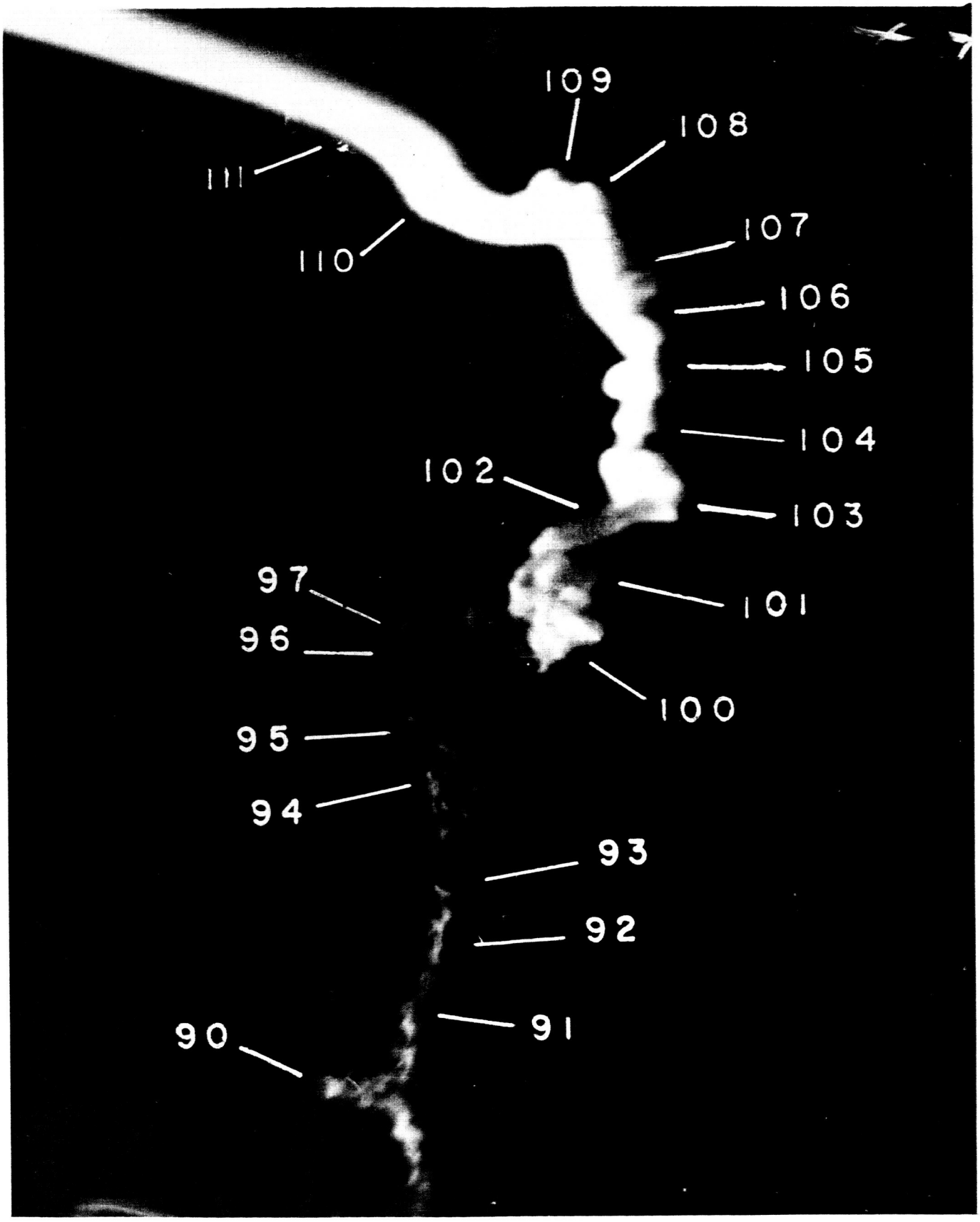
109
108
111
107
110
106
105
104
102
103
97
101
96
100
95
94
93
92
90
91

Figure 1

110 km, and may be present in any part or nearly all of this region. The "stringy" structure appears below the globules in nearly all trails.

The "globules" are usually not observable until the trail is several seconds old. They first appear as small spherical lumps and grow rapidly. If the wind shear is small in the region, as is the case in Figure 1, the spherical shape is maintained while the globule attains a radius of several kilometers. When a shear is present, the initial, nearly spherical, shape of the globule is quickly distorted by the shear, and sometimes forms long plumes, as shown in Figure 2.

The "stringy" region begins at or near the end of the globules; thus, its upper limit varies for different trails. The effect of the absence or presence of wind shear on this portion of the trail may also be seen in Figures 1 and 2. The strings expand at a rapid rate like the globules, and the trails generally fade quickly. The rapid fading is thought to be largely due to chemical consumption at the lower heights. Below about 80 km, trails of sodium vapor appear white and do not have the characteristic yellow color of the D-lines that illuminates the upper trail. This indicates that chemical consumption of the atomic vapor is very rapid below that altitude.

B. DEFINITION AND CRITERION OF TURBULENCE

It is apparent that a complete statistical theory of turbulence which can be directly applied to the upper atmosphere does not exist at the present. The mathematical difficulties of a general solution to the problem have led investigators to vary the method of approach as well as the form of

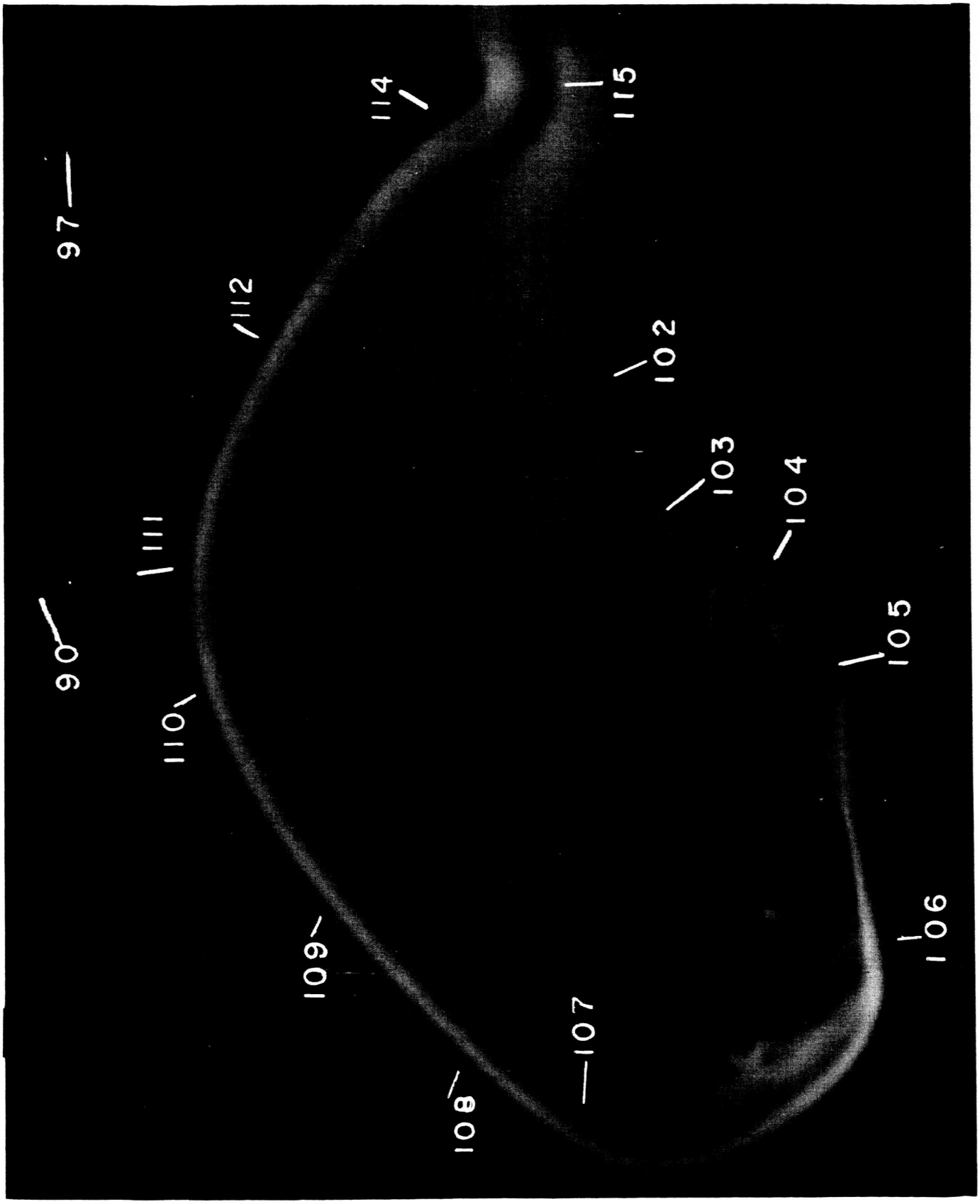

Figure 2

the necessary simplifying assumptions and thus the conclusions as to the conditions for the existence of turbulence and its exact character. However, most studies are based on the concept originally developed by Kolmogoroff. Basically this concept states that for sufficiently high values of the Reynolds number, all turbulent motion has the same sort of isotropic and statistically uniform small scale structure. Energy from the mean flow is transferred to a spectrum of eddies having effective wavelengths which vary from those characteristic of the mean flow down to a lower limit where energy is absorbed into the random heat motion of the molecules by viscosity.

The maintenance of a turbulent regime is generally considered to be completely dependent on the value of the Richardson number. The value of this number depends directly on the wind shear in the mean flow which is an observable quantity. The only other observable quantity is the expansion rate of the trails. Kolmogoroff formulated two similarity hypotheses:

1. The statistical characteristics of the turbulent motion depends only on the mean energy dissipation per unit mass of fluid and on viscosity.

2. The statistical character of the larger eddies depends only upon the rate of energy dissipation.

From these hypotheses certain predictions concerning the expansion rates can be derived.

1. For Small Times $= \left[r^2 - r_o^2\right] \sim T^2$
2. For Intermediate Times $= \left[r^2 \sim T^3\right]$

C. OBSERVATIONS

1. Wind Shear

Observations[4] of 30 vapor trails during twilight show that wind shears as great as 100 m/sec/km may be present at times in narrow regions around 100 km. However, shears greater than about 50 m/sec/km are not frequent. Shears of 20 to 30 m/sec/km are usually present, but at times no observable shear exists. The globules extended to 111 km in some trails and were absent or not detectable in others. The occurrence of the globules appears to be independent of wind shear. One third of the observations occurred when the shear was less than 10 m/sec. Most of the remaining irregular regions were affected by shears of between 20 and 40 m/sec/km.

The value of the Richardson number required to maintain turbulence at this altitude is difficult to determine exactly. Values of 1/2 to 1/25[5] have been suggested. The low values infer wind shears of at least 100 m/sec/km. Such shears are occasionally observed, but only a few approaching this value are associated with the trail irregularities reported here. The wide range of uncertainty in the critical value of the Richardson number prevents it from being a conclusive argument either for or against the existence of turbulence around 100 km.

2. Expansion Rate of Trails

That the irregular portions of the trails expand more rapidly than expected from molecular depression is apparent from visual observation. Most trails have an obviously smaller diameter just above the irregular region.

TABLE II

GROWTH RATE OF
IRREGULAR TRAILS

Date	Height (km)	Growth Rate (m/sec)
2 March 1962	80.4	1.6
	85	1.1
	93.3	2.6
	95	4.4
	96	2.2
	97.6	3.2
	100.5	5.0
	101.9	3.6
	104.3	3.8
17 April 1962	93	2.7
	94	4.1*
	102	4.8
	105	3.6
22 May 1963 AM	98.1	4.1
	98.1	4.1
16 Jan 1964	95	3.4
	102.2	3.55
	102.6	3.65
	104	4.7
	104	5.5*
	107	5.5*
	109	3.35*

* Measurement on a Specific Globule.

However, an exact measure of the expansion rate is often difficult. Wind shear distorts many trails and produces an uncertainty in the location of the trail edge especially when measurements are required for a long period. Uneven illumination of an optically dense trail, changing sky background, variable exposure time, and unfavorable camera angle all prevent accurate measurement of expansion rates of some trails.

Through careful selection of photographs to minimize some of the difficulties, it was possible to measure accurately the radius of certain trails for varying intervals of time. Some of these measurements are shown in Figures 3 and 4. The radius of the trails is plotted as a function of the time after ejection of the vapor. The height of the observed region, the date, the observing site, and the focal length of the recording camera are also shown. The radius of the trails increases linearly with time at a rate of 2 to 5 m/sec. A summary of expansion rates at various altitudes from four selected trails are recorded in Table II. The asterisk indicates that the measurement was made on a specific "globule". The other measurements were made between "globules" or on the lower "stringy" portion of the trail: The expansion rate below 95 km is usually less than 3 m/sec and is greater above that height.

D. SUMMARY

The rapid growth of symmetrical globules without change of shape is highly uncharacteristic of turbulence as described. The occurrence of fully developed irregularities in regions of very low shear requires a different mechanism for the transfer of turbulent energy. The observed expansion rates

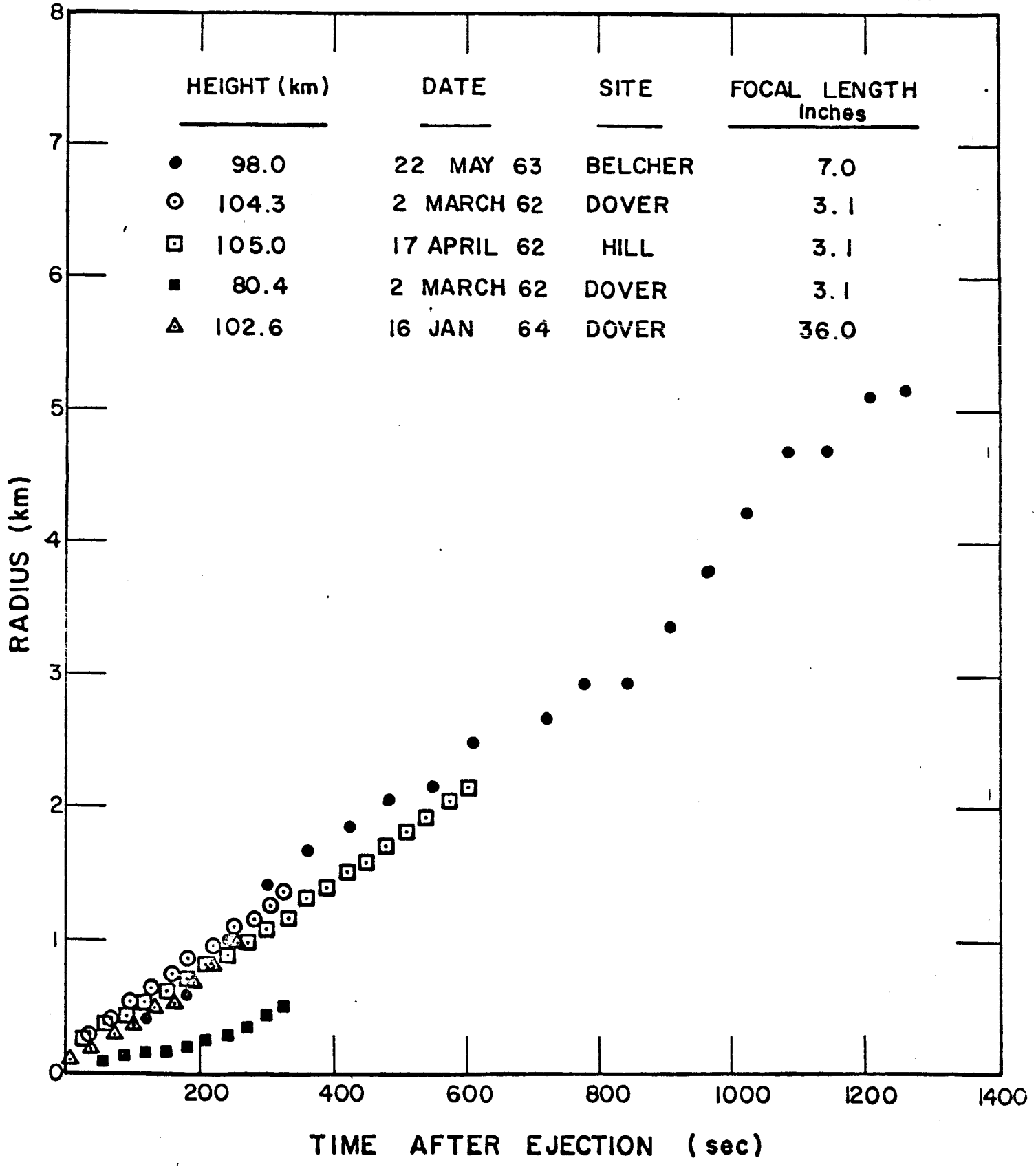
HEIGHT (km)
DATE
SITE
FOCAL LENGTH Inches
98.0 22 MAY 63 BELCHER 7.0
104.3 2 MARCH 62 DOVER 3.1
105.0 17 APRIL 62 HILL 3.1
80.4 2 MARCH 62 DOVER 3.1
102.6 16 JAN 64 DOVER 36.0
RADIUS (km)
0
1
2
3
4
5
6
7
8
200
400
600
800
1000
1200
1400
TIME AFTER EJECTION (sec)

Figure 3

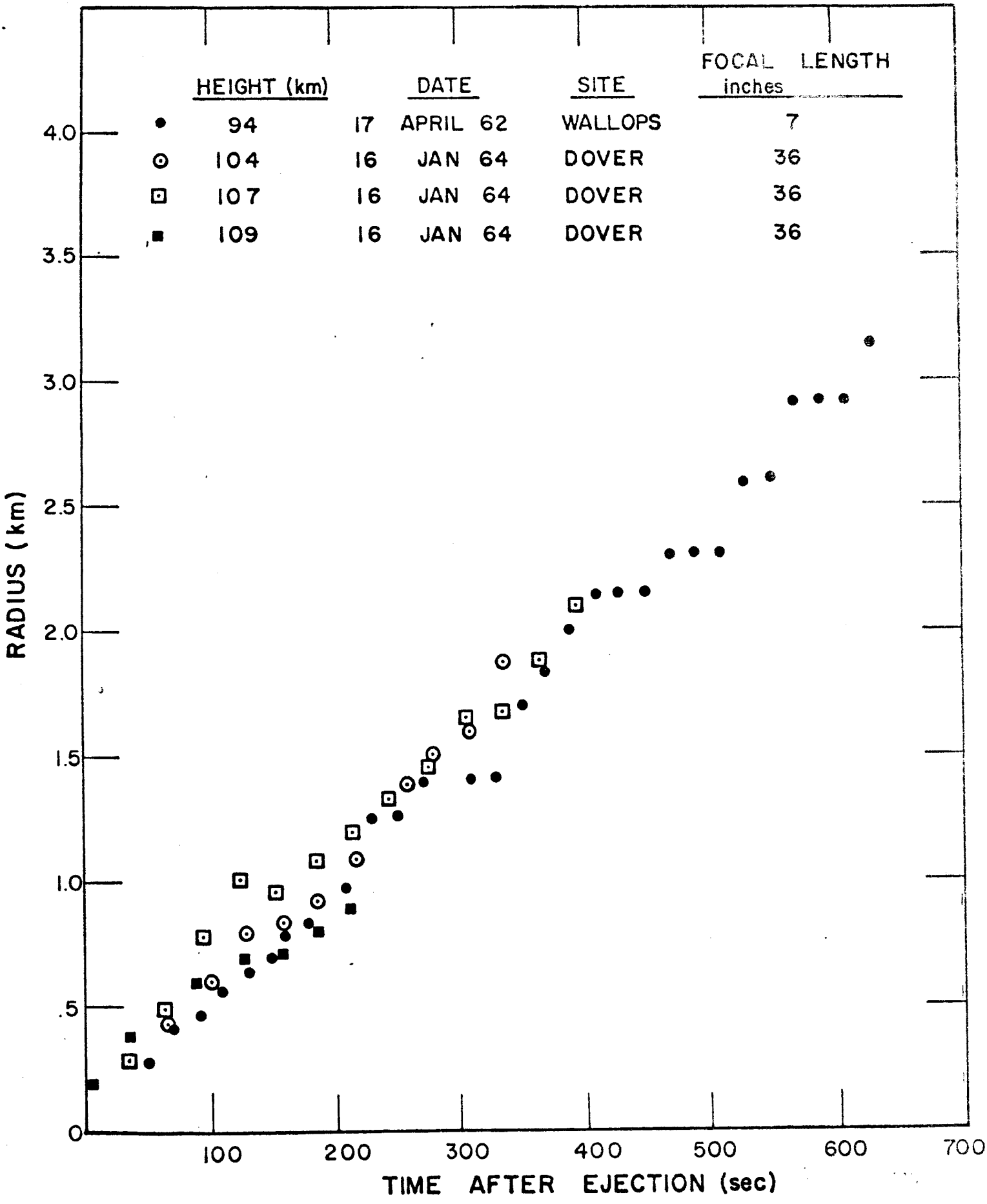
HEIGHT (km)
DATE
SITE
FOCAL LENGTH inches
94 17 APRIL 62 WALLOPS 7
104 16 JAN 64 DOVER 36
107 16 JAN 64 DOVER 36
109 16 JAN 64 DOVER 36
RADIUS (km)
TIME AFTER EJECTION (sec)
0
.5
1.0
1.5
2.0
2.5
3.0
3.5
4.0
100
200
300
400
500
600
700

Figure 4

are not predicted by existing theories of turbulence. Thus one must conclude that the irregularities present on most vapor trails are not conclusive evidence of pre-existing turbulence in the atmosphere. Of course, this does not preclude the possibility that the dynamics of the atmosphere are responsible in a manner not yet understood. Another possibility is that the disturbance is in some way connected with the formation of the trail. In fact, some evidence supports such a conclusion. The irregularities occur only on the upward trail from Wallops Island when the vapor is being ejected vigorously, but not on the down trail when rapid burning of the vaporizer ends before reaching the 100 km level. Other investigators[2] have reported the phenomenon on both the up and down portions of the trajectory when vapor ejection was rigorous at both times. Irregularities in quantity and energy of the ejected vapor as well as disturbances due to the passage of the rocket vehicle certainly occur but cannot explain the rapid and persistent growth rate.

The lower part of the "stringy" portion is affected by chemical reactions, as evidenced by the character of the trail brightness. The entire upper region in which the trail is irregular is also very active chemically. Various materials ejected into this height region at night have produced bright and persistent trails due to photochemical reactions. As in other phenomena, the interpretation of irregular structure of ejected vapor trails requires more understanding of the 100 km region of the earth's atmosphere than is presently available.

V. FUTURE PLANS

It is expected that the next series of rocket firings will occur about the middle of January at Wallops Island. After the firings, reduction and analysis of data will begin and continue through the next reporting period.

REFERENCES

1. Manring, E. R., Bedinger, J. F., and Knaflich, H., Space Research II, ed. by van de Hulst, H. C., de Jager, C. and Moore, A. F., N. Y. Industrial Publishers, Inc., 1107-1124 (1961).

2. Blamont, J. and de Jager, C., Am. Geophys. 17, 134-144 (1961).

3. Gallet, R. M., Proc. Inst. Radio Engr. 43, 1240, (1955).

4. Bedinger, J. F., and Knaflich, H., Seminar on Sporadic E, Estes Park, Colo., June 1965, to be published in Radio Science.

5. Layzer, D., "Ionosphere Sporadic E", Vol. II, Pegamon Press LTD.